Journal of Power Sources 188 (2009) 502–506

Contents lists available at ScienceDirect

Journal of Power Sources

journal homepage: www.elsevier.com/locate/jpowsour

Short communication

MEA for alkaline direct ethanol fuel cell with alkali doped PBI membrane and non-platinum electrodes

A.D. Modestov[a,*], M.R. Tarasevich[a,b], A. Yu. Leykin[b], V.Ya. Filimonov[a]

[a] A.N. Frumkin Institute of Physical Chemistry and Electrochemistry, Russian Academy of Sciences, Leninsky prospect 31, 119991 Moscow, Russia
[b] National Innovation Company "New Energy Projects", Prechistenka Street 18, 119034 Moscow, Russia

ARTICLE INFO

Article history:
Received 15 July 2008
Received in revised form 7 November 2008
Accepted 28 November 2008
Available online 6 December 2008

Keywords:
PBI
Direct ethanol fuel cell
Alkaline fuel cell

ABSTRACT

This paper reports on the fabrication of MEA for alkaline direct ethanol fuel cell (ADEFC). The MEA was fabricated using non-platinum electrocatalysts and a membrane of alkali doped polybenzimidazole (PBI). The employed oxygen reduction catalyst was prepared by pyrolysis of 5,10,15,20-tetrakis(4-methoxyphenyl)-21H,23H-porphine cobalt(II) supported on XC72 carbon. This catalyst is tolerant to ethanol. Electrocatalyst at the anode was RuV alloy supported on XC72 carbon. It was synthesized by reduction of respective salts at elevated temperature. Single cell power density of 100 mW cm^{-2} at $U = 0.4$ V was achieved at 80 °C using air at ambient pressure and 3 M KOH + 2 M EtOH anode feed. The developed MEA is considered viable for use in emergency power supply units and in power sources for portable electronic equipment.

1. Introduction

Alkaline direct ethanol fuel cell (ADEFC) is developed as a small to medium scale emergency power supply unit and an alternative power source for small scale applications such as mobile phones, laptops, etc. [1,2]. Ethanol is a non-toxic fuel which can be produced in an environment friendly way by fermentation of sugar-containing plant materials. Complete oxidation of ethanol to form carbon dioxide is a 12-electron process:

$$C_2H_5OH + 12OH^- - 12e^- \rightarrow 2CO_2 + 9H_2O \quad \text{(anode)}$$

$$3O_2 + 6H_2O + 12e^- \rightarrow 12OH^- \quad \text{(cathode)}$$

$$C_2H_5OH + 3O_2 + \rightarrow 2CO_2 + 3H_2O \quad (1)$$

The real ethanol oxidation path depends on the anode catalyst, electrode potential, electrolyte composition and pH, and other parameters. Standard potential of ethanol oxidation is only 0.084 V lower than the standard potential of hydrogen electrode [3,4]. Oxidation of ethanol is a complex multistage process. Reaction is hindered by poisoning of Pt anodes by ethanol oxidation intermediates. Use of platinum alloys, such as PtSn, helped improve the performance of anodes in acidic media [5–7]. In acidic environment of proton exchange membranes the main products of ethanol electrochemical oxidation at Pt based electrodes are acetaldehyde and acetic acid (two- and four-electron oxidation processes, respectively) [3,7–11], the yield of carbon dioxide is only 8–9%. However, even with the use of pressurized oxygen (0.2 MPa) the maximal power density of the fuel cell remains rather small (80 mW cm^{-2}) [12]. The rate of electrochemical oxidation of ethanol in alkaline solutions is higher than in acidic media due to less pronounced poisoning of the anodes [8]. Compared to acidic media, in alkaline solutions oxygen reduction electrocatalysts are characterized by increased rate of oxygen reduction and higher corrosion stability. For this reason even non-platinum oxygen reduction catalysts can be used in ADEFC [13–15]. However, with the employment of platinum alloy catalysts (PtRu, PtSn, PtRh, PtW, PtMo) the carbon dioxide yield remained small. The drawback of the use of alkaline media in fuel cell is the neutralization of alkali by products of ethanol oxidation - carbon dioxide and acetic acid. For this reason aqueous alkaline solution of alcohol should be supplied to the anode [16]. The use of cation exchange membranes in ADEFC is objectionable because of production and precipitation of alkali at the cathode. Present anion exchange membranes suffer from both poor ionic conductivity and low chemical stability [13,17]. The use of alkali-doped PBI membranes in hydrogen-oxygen FC was proposed in [18]. PBI stands for a family name of a group of outstandingly thermally resistant polymers. These polymers are characterized by exceptional chemical stability both in alkaline and in acidic media. Pure PBI is an excellent electric insulator. However, PBI swells in contact with strong acids or alkali, acquiring ionic conductivity. This process if often called doping of PBI. Ionic conductivity of PBI doped with potassium hydroxide can be as high as 10^{-1} S cm^{-1} [18–20].

Membranes of phosphoric acid doped PBI were tried in [21] for oxidation of ethanol at 175 °C, although power density of the

* Corresponding author. Tel.: +7 495 9522387; fax: +7 495 9525308.
E-mail address: modestov@elchem.ac.ru (A.D. Modestov).

0378-7753/$ – see front matter © 2008 Elsevier B.V. All rights reserved.
doi:10.1016/j.jpowsour.2008.11.118

cell was low. In [2] KOH doped PBI membrane was used to assemble MEA of ADEFC. In that work power density of the single cell reached 60 mW cm^{-2} at 90 °C. Pressurized oxygen (0.2 MPa), PtRu (2 mg cm^{-2}) anodes and Pt (1 mg cm^{-2}) cathodes were used.

To the best of our knowledge, no study focusing on ionic transport in KOH doped PBI has been published. We assume that the transference number of hydroxide ions in the KOH doped PBI matrix remains about the same as in pure aqueous KOH, namely 0.73 [22]. According to Eq. (1), to oxidize completely one molecule of ethanol by removal of 12 electrons, 12 OH^- ions should be provided to the anode. Only about $12 \times 0.73 = 8.76$ OH^- ions are driven from cathode through the membrane to the anode by current passage. It implies that molar concentration of alkali in the anode feed should be at least 3-fold higher than ethanol concentration.

A new group of non-platinum catalysts for ethanol electrooxidation in alkaline media has been synthesized recently in our laboratory [23–25]. They include RuV, RuCr, and RuNi alloys supported on carbon black. It was shown that the main ethanol oxidation products on RuV catalyst in hot alkaline electrolyte are gaseous carbon dioxide and acetate ions. Non-platinum oxygen reduction catalysts produced by pyrolysis of porphyrins supported on carbon black are highly active in alkaline media [24,25]. Another advantage of these catalysts is very low ethanol oxidation rate. It makes these catalysts nearly insensitive to ethanol crossover.

The goal of the work was to devise an effective and relatively cheap MEA for ADEFC. To reach the goal alkali doped PBI film and non-platinum catalysts for ethanol oxidation and oxygen reduction developed in our laboratory were used.

2. Experimental

2.1. Membrane

Poly[2,2′-diphenyloxide-5,5′-bibenzimidazole] was used as the membrane material:

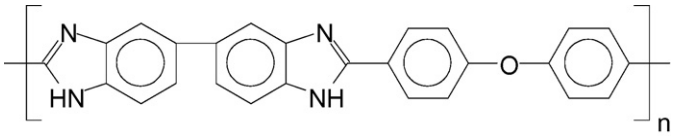

Synthesis, doping and permeability of thin films of poly[2,2′-diphenyloxide-5,5′-bibenzimidazole] (PBI) by ethanol and alkali are addressed elsewhere [26]. 25 μm thick films of PBI were used to prepare membranes. After doping in aqueous 3 M KOH + 2 M EtOH for 48 h at room temperature, 25 μm thick films swelled up to ~30 μm thick. The predoped membranes were used to assemble MEAs only in the first experiments of this study. Later it was found that the stage of the initial doping of the PBI films was redundant. In subsequent tests MEAs were assembled using pristine PBI films. Doping of the pristine PBI within MEAs was accomplished in the test rig during the initial stage of the cell conditioning when the 3 M KOH + 2 M EtOH electrolyte was pumped through the anode compartment of the cell.

2.2. Ethanol oxidation catalyst

RuV carbon supported catalyst was synthesized by high temperature route [23–25]. XC72 carbon black was sonicated in aqueous solution containing $VOSO_4 \times n$ H_2O and $Ru(OH)Cl_3$. After drying in air the resultant powder was heat treated in hydrogen atmosphere at 400 °C for 2 h. The molar ratio of metals in the catalyst was Ru:V = 3:2. The metal (Ru + V) loading in the catalyst was 20% or 40%. X-ray diffraction pattern of the catalyst powder was obtained with a Rigaku D/MAX 2200 diffractometer using Cu $K\alpha$ radiation ($\lambda = 1.5406$ Å). Scans were carried out at 1° min^{-1} for 2θ values ranging between 10° and 100°. Transmission electron microscopy investigations were performed using a Philips EM 301 instrument.

2.3. Oxygen reduction catalyst

Non-platinum oxygen reduction catalyst (TMPhP/C) was synthesized according to procedure reported elsewhere [24,25]. XC72 carbon was added to the solution of 5,10,15,20-tetrakis(4-methoxyphenyl)-21H,23H-porphine cobalt(II) (TMPhP Co) (Sigma–Aldrich) in $CHCl_3$ under continuous stirring. The resultant slurry was sonicated for 2 h at room temperature. The TMPhP Co to carbon support mass ratio before heat treatment was 0.3–1. After drying the powder was baked in Ar atmosphere for 2 h at 850 °C. In some cases Pt (40%)/C oxygen reduction catalyst from E-TEK (USA) was used.

2.4. MEA preparation

Anode catalyst ink was prepared by sonicating aqueous solution of Fumion® ionomer (FumaTech, Germany) with the RuV/C catalyst powder for 30 min. The ionomer was used as a catalyst binder only. The loading of the ionomer was 5% with respect to catalyst. The ink was sprayed on the surface of Toray TGP-H-120 carbon paper.

The cathode catalyst layer was spray coated on the Sigracet 10DC gas diffusion layer (SGL, Germany). Ink was prepared by sonication for 30 min of aqueous suspension of catalyst and FEP 121A emulsion (Electrochem, Inc. USA). The cathodes were tempered at 360 °C for 20 min in Ar atmosphere. Aqueous KOH, which arrived at the cathode by the membrane crossover, supported the ionic current in the cathode catalyst layer. Teflon (FEP) was included in the composition of the cathode catalyst layer in order to control its flooding.

The MEA was formed by placing the PBI membrane between the corresponding electrodes. With the help of PTFE seals the MEA was fixed between the graphite flow fields in the 5 cm^2 single cell fixtures from Electrochem Inc. To start the cell, the preheated aqueous 3 M KOH + 2 M EtOH solution was pumped though the anode compartment, air was supplied to the cathode, the cell temperature was raised using electrical heaters attached to the end plates of the FC fixture. When the cell temperature arrived at the preset value, the voltammetry measurements were started. Usually it took about 50 min to stabilize the cell temperature at 80 °C. Additional 1 h was required to obtain reproducible voltammetry curves.

2.5. MEA testing

Flow (5 ml min^{-1}) of aqueous electrolyte 3 M KOH + 2 M EtOH preheated to the test temperature was supplied by peristaltic pump to the anode compartment of the single cell. The cathode compartment was supplied with 0.2 l min^{-1} flow of air or oxygen. In some cases air (oxygen) was humidified by passing through the deionized water filled bubblers, which were held at the cell temperature. Since no influence of air (oxygen) humidification was observed, most of the experiments were performed using ambient air (oxygen) without humidification. The single cell was controlled using IPC Pro M 3A potentiostat/galvanostat (Russia). The voltammetry curves were measured in both scan directions at 2 mV s^{-1} voltage ramp rate.

3. Results and discussion

Fig. 1 shows the diffraction pattern of the RuV/C catalyst. The diffraction pattern for the carbon-supported catalyst shows two broad Bragg peaks. The peak at $2\theta = 25°$ is assigned to the (0 0 2) diffraction of the graphitic portion of XC72 carbon. The second peak, centered around $2\theta = 43°$, can be attributed to either the reflections from (1 1 0) planes of RuV compound or to reflections from

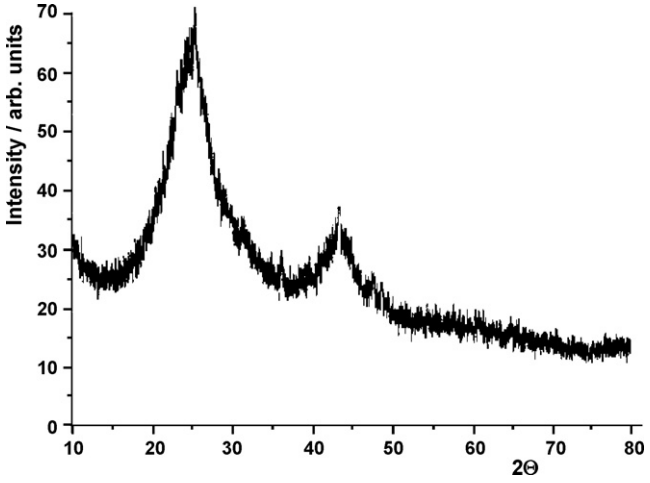

Fig. 1. X-ray diffraction pattern of the 20% RuV/C catalyst.

(1 0 1) planes of Ru lattice. Crystal structure of RuV is cubic (CsCl-type, $a = 3.003$ Å, $2\theta = 42.715^\circ$) [27]. The XRD pattern of ruthenium exhibit strongest peak at $2\theta = 44.004^\circ$ which is due to reflections from (1 0 1) planes of hexagonal lattice [27]. Deformation of the ruthenium lattice caused by incorporation of vanadium atoms can be the reason for the diffraction peak shift to lower 2θ values. The diffraction peak is apparently broadened by low crystallinity and smallness of the catalyst particles.

Representative TEM image of the 20% RuV catalyst, as displayed in Fig. 2, revealed poorly crystalline particles in the 2–6 nm size range.

Performance of the ADEFC single Cell (I) is shown in Fig. 3. The MEA of the Cell (I) was assembled with cathode, comprising Pt/C catalyst in the active layer, and anode in which 20% RuV/C catalyst was used. The FEP loading in the cathode active layer was 50% of carbon support. These measurements were used as a benchmark. Platinum loading at the cathode was 1.24 mg cm^{-2}. Metal (Ru + V) loading in the anode catalyst layer was 2.1 mg cm^{-2}. Experiments were performed at 80 °C. In this figure and in the following, curve "A" represents voltage dependence on current density (U–j), while curve "B" shows power density (P) dependence on current density. The insert in Fig. 3 shows the slow decrease of current density when the cell voltage was fixed at 0.5 V. The value of the single cell power density reached 90 mW cm^{-2} at 0.4 V. When air, supplied to the cathode, was replaced by pure oxygen, the power density value at 0.4 V increased up to 110 mW cm^{-2} (not shown).

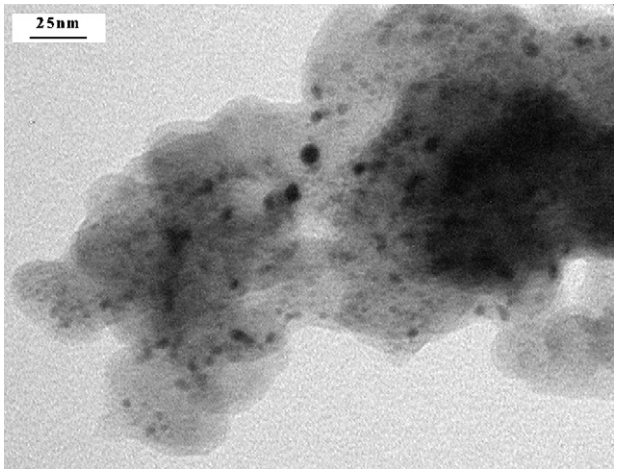

Fig. 2. TEM image of the 20% RuV/C catalyst.

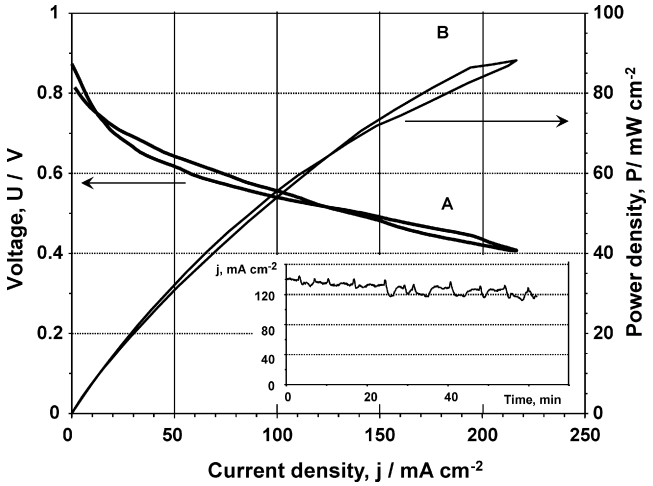

Fig. 3. Performance of Cell (I) at 80 °C: feed – ambient air, 3 M KOH + 2 M EtOH; anode – RuV/C loading (metals) – 2.1 mg cm^{-2}; cathode – Pt/C, loading (Pt) – 1.24 mg cm^{-2}.

Performance of the Cell (II) is shown in Fig. 4. In this case the MEA was assembled using only non-platinum catalysts. Loading of the TMPhP/C oxygen reduction catalyst at the cathode was 9.2 mg cm^{-2}, FEP to catalyst mass ratio was 1:1. In the anode, catalyst layer comprised 40% RuV/C catalyst. The loading (Ru + V) was 4.5 mg cm^{-2}. Comparison of data presented in Figs. 3 and 4 shows that the replacement of Pt by the non-platinum TMPhP/C oxygen reduction catalyst at the cathode did not compromise the cell performance. The insert in Fig. 4 shows that at the fixed cell voltage, $U = 0.5$ V, current density value was stabilized after a period of about 10 min. Replacement of air by oxygen in the cathode feed resulted in about 10% increase of current density, curves "A, Air" and "A, O_2" in Fig. 4, respectively. Apparently the cell performance can be improved by refinement of the anode. Substantial hysteresis of U–j curves is observed in Fig. 4. The hysteresis was diminished by the increase of the electrolyte pumping rate up to 20 ml min^{-1} (not shown).

Fig. 5 shows performance of the single Cell (III) with reduced loading of the RuV/C ethanol oxidation catalyst. The loading (Ru + V) was reduced by more than 6 times, down to 0.72 mg cm^{-2}. The cathode of the Cell (III) was virtually identical to the cathode used in Cell (II). It contained TMPhP/C oxygen reduction catalyst - 9 mg cm^{-2}. Measurements were performed at 80 °C. The insert in Fig. 5 shows the stability of current density when cell voltage was fixed at 0.6 V.

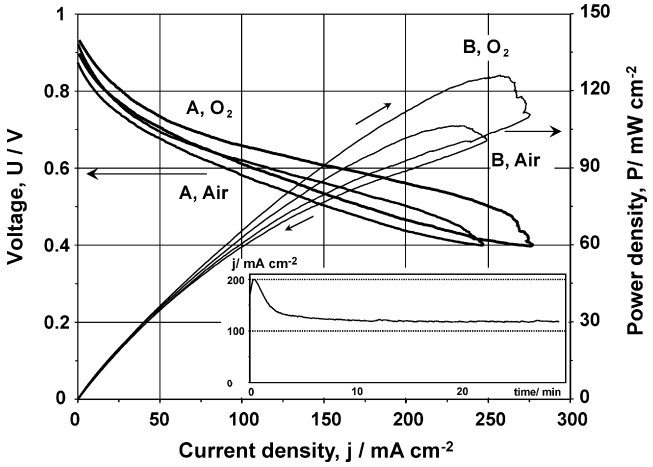

Fig. 4. Performance of Cell (II) with non-platinum electrodes at 80 °C: feed – ambient air or oxygen, 3 M KOH + 2 M EtOH; catalyst layers: cathode – TMPhP/C – 9.2 mg cm^{-2}, anode – RuV/C loading (Ru + V) – 4.5 mg cm^{-2}.

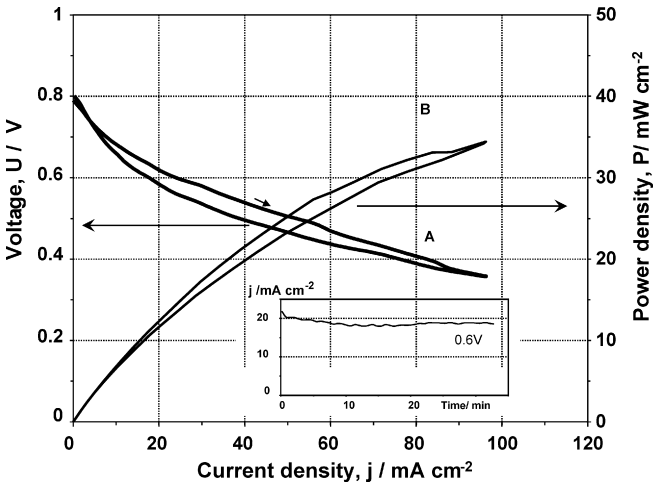

Fig. 5. Performance Cell (III) with non-platinum electrodes at 80 °C: feed – ambient air, 3 M KOH + 2 M EtOH; anode – RuV/C loading (Ru + V) –0.72 mg cm^{-2}; cathode – TMPhP/C – 9 mg cm^{-2}.

The maximal power density of the single cell reached 35 mW cm^{-2} at 0.35 V. Comparison of the performance of Cell (II) and Cell (III) shows that the about 6-fold decrease in the (Ru + V) loading in the anode resulted in approximately 4-fold drop of current density, e.g. at U = 0.4 V.

We tried to increase the ADEFC performance by the increase of the RuV/C loading at the anode above 4.5 mg cm^{-2}. The use of higher RuV/C loading, (Ru + V) 8 mg cm^{-2}, at the anode did not help improve the cell performance compared to the performance of the Cell (II) (results are not shown). Apparently at high anode catalyst loading (Ru + V), 4.5 mg cm^{-2} and higher, the anode performance is limited by the sluggish diffusion of ethanol and/or its oxidation products within the thickness of the anode catalyst layer. On the other hand, it implies that the loading of the oxygen reduction catalyst could be reduced without significant loss of performance. Replacement of air by oxygen in the cathode feed of Cell (III) increased current density at 0.35 V only by ~5% (not shown).

The performance of the single cells tested, Cells (I)–(III), was high. However it was limited by the low rate of ethanol oxidation at the anode regardless of the loading of the RuV/C catalyst at the anodes. It indicates that the further improvement of the ADEFC performance with RuV/C and TMPhP/C catalysts at the electrodes requires substantial refinement of the structure of the anode catalyst layer.

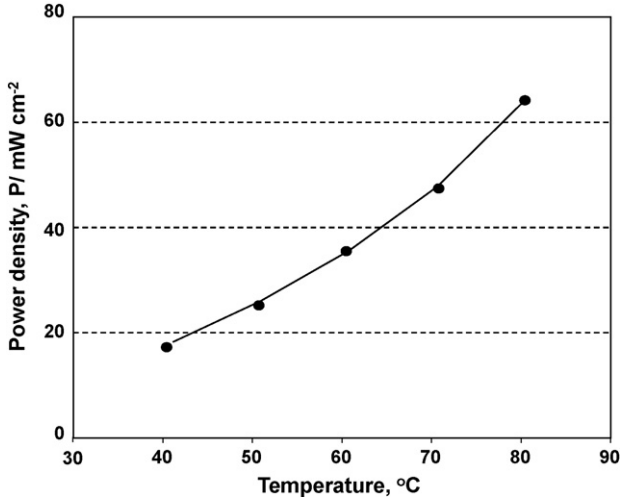

Fig. 6. Temperature dependence of power density of Cell (IV) with non-platinum electrodes: feed – 3 M KOH + 2 M EtOH, ambient air; anode – RuV/C loading (Ru + V) – 0.88 mg cm^{-2}; cathode – TMPhP/C – 7.1 mg cm^{-2}. Readings were taken at U = 0.4 V.

Operational readiness of the small scale power source depends on its ability to deliver power at ambient temperature so that the power could be used to reach the working temperature range. Temperature dependence of current density of single cell with non-platinum electrocatalysts is shown in Fig. 6. This sequence of measurements was performed using Cell (IV). Anode catalyst layer of this cell comprised RuV/C catalyst, while at the cathode TMPhP/C oxygen reduction catalyst was used (FEP/catalyst ratio 1:1). Series of voltammetry measurements were performed at temperatures 40, 50, 60 70 and 80 °C. The power density readings at cell voltage 0.4 V were taken from the respective U–j curves. These readings are plotted versus temperature. According to Fig. 6, single cell performance sharply increases with the temperature raise.

4. Conclusions

1. High power density MEA for alkaline direct ethanol fuel cell was devised using non-platinum catalysts at both electrodes and KOH doped PBI membrane.
2. Power density of the single cell fed with air at ambient pressure reached 100 mW cm^{-2}. Reported performance of the ADEFC single cell is substantially higher than recently published data on the ADEFC, which employed Pt and PtRu based electrodes and KOH/PBI membrane (60 mW cm^{-2}, 90 °C, oxygen at 0.2 MPa) [2].
3. Swelling (doping) of 25 μm thick poly[2,2′-diphenyloxide-5,5′-bibenzimidazole] (PBI) membranes in 3 M KOH + 2 M EtOH was found to be quite fast. It enabled us to fabricate MEAs using pristine PBI films. Doping of PBI films to form ion conducting membranes was accomplished during the period of the cell conditioning. It facilitates the MEA fabrication procedure.
4. Performance of our ADEFC is limited by the processes occurring at the anode. At high catalyst loading at the anode transport of ethanol and/or its oxidation products is the limiting stage. Performance can be improved by the refinement of the structure of the anode catalyst layer.
5. The use of non-platinum catalysts and high performance of single cell makes the MEA viable as a core of small scale power source.

Acknowledgement

This work was supported by the "New Energy Projects" National Innovation Company, Russia.

References

[1] A. Verma, S. Basu, J. Power Sources 145 (2005) 282.
[2] H. Hou, G. Sun, R. He, Z. Wu, B. Sun, J. Power Sources 182 (2008) 95.
[3] C. Lamy, A. Lima, V. LeRhun, F. Delime, C. Countanceu, J.-M. Léger, J. Power Sources 105 (2002) 283.
[4] R. Chetty, K. Scott, Electrochim. Acta 52 (2007) 4073.
[5] C. Lamy, S. Rousseau, E.M. Belgsir, C. Counteceau, J.-M. Léger, Electrochim. Acta 49 (2004) 3901.
[6] Guangchun Li, P. G. Pickup, Electrochimica Acta 52 (2006) 1033.
[7] F. Vigier, S. Rousseau, C. Coutanceau, J.-M. Léger, C. Lamy, Top. Catal. 40 (2006) 111.
[8] L. Colmenares, H. Wang, Z. Jusys, L. Jiang, S. Yan, G.Q. Sun, R.J. Behm, Electrochim. Acta 52 (2006) 221.
[9] H. Wang, Z. Jusys, R.J. Behm, J. Phys. Chem. B 108 (2004) 19413.
[10] J.F.E. Gootzen, W. Visscher, J.A.R. van Veen, Langmuir 12 (1996) 5076–5082.
[11] H. Wang, Z. Jusys, R.J. Behm, Fuel cells 4 (2004) 113.
[12] L. Jiang, G. Sun, S. Sun, J. Liu, S. Tang, H. Li, B. Zhou, Q. Xin, Electrochim. Acta 50 (2005) 5384.
[13] J.R. Varcoe, R.C.T. Slade, G.L. Wright, Y. Chen, J. Phys. Chem. B 110 (2006) 21041.
[14] C. Tamain, S.D. Poynton, R.C.T. Slade, B. Carroll, J.R. Varcoe, J. Phys. Chem. C 111 (2007) 18423.
[15] T. Burchardt, P. Gouérec, E. Sanchez-Cortezon, Z. Karichev, J.H. Miners, Fuel 81 (2002) 2151.

[16] C. Coutanceau, L. Demarconnay, C. Lamy, J.-M. Léger, J. Power Sources 156 (2006) 14–19.
[17] J.R. Varcoe, R.C.T. Slade, Fuel Cells 5 (2005) 187.
[18] B. Xing, O. Savadogo, Electrochem. Commun. 2 (2000) 697.
[19] O. Savadogo, J. Power Sources 127 (2004) 135.
[20] J. Roziére, D.J. Jones, M. Marrony, X. Glipa, B. Mula, Solid State Ionics 145 (2001) 61.
[21] J. Wang, S. Wasmus, R.F. Savinell, J. Electrochem. Soc. 142 (1995) 4218.
[22] A.J. Bard, L.R. Faulkner, Electrochemical Methods. Fundamentals and Applications, John Wiley & Sons, INC, New York, 2001, Chapter 2.
[23] M.R. Tarasevich, Z.R. Karichev, V.A. Bogdanovskaya, E.N. Lubnin, A.V. Kapustin, Electrochem. Commun. 7 (2005) 141.
[24] A.Yu. Tsivadze, M.R. Tarasevich, V.N. Andreev, V.A. Bogdanovskaya, B.N. Efremov, N.A. Kapustina, V.N. Titova, A.A. Yavich, N.N. Belova, P.V. Mazin, Int. Sci. J. Alternative Energy Ecol. (2007) 58, N4.
[25] A.Yu. Tsivadze, M.R. Tarasevich, B.N. Efremov, N.A. Kapustina, P.V. Mazin, Doklady Phys. Chem. 415 (2007) 234.
[26] A.Y. Leykin, O.A. Shkrebko, M.R. Tarasevich, J. Membr. Sci 328 (2009) 86–89.
[27] R.M. Waterstrat, R.C. Manuszewski, J. Less-Common Met. 48 (1976) 151.